28th ABCM International Congress of Mechanical Engineering
November 09-14, 2025, Curitiba-PR, Brazil

# COB-2025-0528
# INFLUENCE OF NOZZLE GEOMETRY AND NUMBER ON MASS FLOW RATE AND POTENTIAL CORE OF SUPERSONIC JETS IN BOF CONVERTERS.

**Gabriell Rodrigues de Souza**
**João Filipe Calatrone Albuquerque Filho**
**Renato do Nascimento Siqueira**
**João Paulo Barbosa**
**Lucas Henrique Pagoto Deoclecio**
GPMF, Department of Mechanical Engineering, Federal Institute of Espírito Santo – Campus São Mateus, Rod. BR 101 norte, km 58, Litorâneo, São Mateus, ES, 29932-540, Brazil.
gabriellrodrigues987@gmail.com; jfilipe0108@gmail.com; renatons@ifes.edu.br; jpbarbosa@ifes.edu.br; lucas.deoclecio@ifes.edu.br

**Ayrton Cavallini Zotelle**
Department of Mechanical Engineering, Celso Suckow da Fonseca Tecnology Education Federal Center (Cefet/RJ) – Campus Angra dos Reis, Rua do Areal, 522 - Parque Mambucaba, Angra dos Reis, RJ, 23953-030, Brazil.
ayrton.zotelle@cefet-rj.br

**Breno Totti Maia**
Lumar Metals - South America Rod. MG 232 - Km 09, 70, Santana do Paraíso Minas Gerais, Brasil CEP: 35.179-000, Brazil.
breno.totti@lumarmetals.com.br

**José Roberto de Oliveira**
Department of Metallurgical and Materials Engineering, Federal Institute of Espírito Santo – Campus Vitória, Av. Vitória, 1729 - Jucutuquara, Vitória - ES, 29040-780, Brazil. jroberto@ifes.edu.br.

***Abstract.*** *The efficiency of steel production in Basic Oxygen Furnace (BOF) converters is directly influenced by the dynamics of supersonic oxygen jets, which are governed by nozzle geometry and configuration. This study presents a comprehensive numerical investigation of the effects of nozzle number (three and five) on the mass flow rate and potential core length of supersonic jets under industrially relevant conditions (NPR = 12). Three-dimensional CFD simulations were performed using the* $SST\ k-\omega$ *turbulence model and adaptive mesh refinement, based on experimentally validated geometries and boundary conditions. The results demonstrate that increasing the nozzle pressure ratio (NPR) leads to higher mass flow rates and longer potential cores, with these effects being more pronounced in the three-nozzle configuration. In contrast, the five-nozzle arrangement provides equal total mass flow rate but with a shorter potential core, favoring greater operational control and reduced risk of refractory wear and slopping. The findings provide valuable insights for the optimization of nozzle design and operational parameters in BOF converters, supporting improved productivity, process stability, and equipment durability.*

***Keywords:*** *LD Converter, CFD analysis, BOF, supersonic jet, mass flow rate, CFD, potential core, Three dimensional simulation*

## 1. INTRODUCTION

The supersonic oxygen jet is widely used in the steelmaking process in Basic Oxygen Furnace (BOF) converters, playing a crucial role both in the removal of carbon from the molten metal and in intensifying mixing and chemical reactions during refining (Li *et al.*, 2014). According to studies by Li *et al.* (2014), Feng *et al.* (2021), Garcia *et al.* (2023a), and Zotelle *et al.* (2024), the configuration of the injection nozzles exerts a direct influence on the jet flow patterns, being a determining factor for the efficiency of the metallurgical process. The blow performance in BOF converters depends on several operational and constructive factors of the injection lance. Maia *et al.* (2014) highlights that aspects such as operating height, thermal conditions, oxygen flow rate, and especially the nozzle configuration affect the jet behavior and the refining dynamics. Originally, only one nozzle was used, but to mitigate excessive projections and improve yield, lances with multiple nozzles were developed, currently ranging from four to six Maia *et al.* (2014).

Li *et al.* (2014) point out that the number of nozzles influences both the coalescence of the jets and the metallurgical performance of the converters. Configurations with three to six nozzles are common because they allow greater oxygen flow, reduction of slopping, and less refractory wear. Furthermore, changes in nozzle geometry directly impact the flow patterns, affecting process efficiency. Due to the high temperature and complexity of the environment, many characteristics of the blow are difficult to measure experimentally, which has driven the use of computational simulations. Studies such as those by Alam *et al.* (2010) and Garajau *et al.* (2017) demonstrated good agreement between numerical and experimental results, validating this approach to investigate complex phenomena in the BOF process.

Given this scenario, this work proposes to analyze the influence of the number of nozzles (three and five) on the mass flow rate and the behavior of the supersonic jet under a nozzle pressure ratio (NPR) of 12. The aim is to understand how the variation in the number of nozzles affects the mass flow rate and the length of the potential core, an essential parameter for blow efficiency. A longer potential core can favor greater penetration and stability, optimizing the transfer of momentum and energy to the metal bath. However, excessively long lengths can increase aggressiveness on the converter bottom, raising the risk of localized wear and undesirable projections. Thus, this study aims to provide support for defining more efficient operational parameters and for improving nozzle designs.

For this analysis, three-dimensional simulations were carried out based on real experimental geometries, at reduced scale. To optimize computational performance, the rounded chamfer was simplified by straight edges, preserving mesh continuity and flow fidelity. The simulations were conducted in Ansys Fluent 2025 R1, with symmetry conditions to reduce computational cost, and geometric angles of 120° for three nozzles and 72° for five. The $SST\ k-\omega$ turbulence model was adopted due to its robustness in supersonic flows, and the mesh was adaptively refined in regions of steep gradients and shock waves. The operational parameters reflect typical industrial conditions, ensuring the representativeness of the results and allowing future experimental comparisons.

The numerical simulations performed in this study were previously validated by comparison with experimental data from the literature, demonstrating good agreement in reproducing the main phenomena of supersonic blows in convergent-divergent nozzles. The results indicate that, for the analyzed geometries, increasing the pressure ratio raises the mass flow rate and the length of the jet potential core, with this effect being more pronounced in the three-hole nozzles. Although longer cores favor penetration and metallurgical efficiency, they can also intensify refractory wear and the risk of slopping. On the other hand, five-hole nozzles showed higher total flow and a shorter potential core, resulting in greater operational control and lower risk of damage, desirable characteristics for industrial applications that require stability and durability in the process.

## 2. METHODOLOGY

The methodology employed combines a three-dimensional CFD approach based on the RANS equations with adaptive mesh refinement and Schlieren-based validation. A mesh independence test, following Zotelle *et al.* (2024), ensured the accuracy of the numerical domain. Simulations were performed using the SST $k-\omega$ model, with detailed flow analysis based on Mach contours and velocity fields.

### 2.1 Mathematical Formulation

The analysis of the flow pattern in supersonic jets is a three-dimensional, compressible, turbulent, and steady-state problem. It can be solved using the Reynolds Averaged Navier-Stokes (RANS) model in order to obtain the pressure fields and the average velocity, with the effects of turbulent fluctuations being modeled using the Boussinesq hypothesis to reduce the computational cost. The continuity equation is given by:

$$\nabla \cdot (\rho \mathbf{u}) = 0], \tag{1}$$

where u is the average velocity vector and $\rho$ is the density of the fluid, which, for an ideal gas, is:

$$\rho = \rho_0 \left(1 + \frac{K+1}{2} Ma^2\right)^{\frac{1}{1-K}}, \tag{2}$$

$\rho_0$ is the density of the air at the reference temperature (300 K), K = 1.4 is the ratio between the specific heat of the air at constant pressure (cp) and the specific heat at constant volume (cv), and Ma=|u|/c is the Mach number. The speed of sound is calculated for each cell in the computational domain by $c = \sqrt{KRT}$. $R = \bar{R}/M$ is the specific gas constant, $\bar{R} = 8.31$ kJ/(kmolK) is the universal gas constant for the air, M is the molecular mass of the air, and T is the temperature of the air. The momentum equation is:

$$\nabla \cdot (\rho \mathbf{u} \otimes \mathbf{u}) = -\nabla P + \nabla \cdot \left[(\mu + \mu_t)\left(\nabla \mathbf{u} + \nabla \mathbf{u}^T - \frac{2}{3}\nabla \cdot \mathbf{u}\mathbf{I}\right) - \frac{2}{3}\rho k \mathbf{I}\right], \tag{3}$$

In the above equation, $P$ is the pressure field, $\mu$ and $\mu_t$ are the molecular and turbulent thermal conductivity, respectively, and $k = (u' \cdot u')/2$ is the turbulent kinetic energy. The velocity field is determined by solving the energy equation (Eq. 4) throughout the numerical domain:

$$\nabla \cdot [u(\rho E + P)] = \nabla \cdot \left[ (\lambda + \lambda_t) \nabla T + \mu \left( \nabla u + \nabla u^T - \frac{2}{3} \nabla \cdot u\mathbf{I} \right) \cdot u \right], \tag{4}$$

where $E = c_p T - P/\rho + |u|^5/2$; $\lambda$ and $\lambda_t$ are the molecular and turbulent thermal conductivity, respectively.

The turbulent viscosity ($\mu_t$) and the turbulent thermal conductivity ($\lambda_t$) were obtained by applying the turbulence closure model ( Eq.5 and Eq.6 ). The SST (Shear Stress Transport) $k$–$\omega$ model is widely used in the literature to simulate supersonic flows in Laval nozzles (Li *et al.*, 2015, Hadjadj *et al.*, 2015, Yaravintelimath *et al.*, 2016, Garcia *et al.*, 2023b) and was also used in this work. The model was developed by Menter (1994) and has hybrid characteristics that suit simulations with the most adverse pressure gradients and presence of walls, using the robust accuracy of the $k$–$\omega$ model in regions close to walls and the $k$–$\varepsilon$ model for regions of potential flow (ans, 2024). In this model, the turbulent viscosity is given by $\mu_t = \rho\sigma_k k/\omega$, where $\sigma_k$ is a model constant, and the thermal conductivity is $\lambda_t = \lambda\mu_t/\mu$. The turbulence model equations are the turbulent kinetic energy ($k$) equation:

$$\nabla \cdot (\rho u k) = \nabla \cdot \left[ \left( \mu + \frac{\mu_t}{\sigma_k} \right) \nabla k \right] + G_k - Y_k, \tag{5}$$

and the specific dissipation rate ($\omega$) equation:

$$\nabla \cdot (\rho u \omega) = \nabla \cdot \left[ \left( \mu + \frac{\mu_t}{\sigma_\omega} \right) \nabla \omega \right] + G_\omega - Y_\omega + D_\omega. \tag{6}$$

For these equations, $\sigma_k$ and $\sigma_\omega$ are empirical constants. $G_k$ is the production of turbulent kinetic energy, $G_\omega$ is the generation of $\omega$, $Y_k$ and $Y_\omega$ the dissipation of $k$ and $\omega$ due to turbulence and $D_\omega$ represents the cross-diffusion term. The constants used ($\sigma_k$, $\sigma_\omega$ and $c_\omega$) were the ANSYS Fluent default values, ans 2024).

An essential description for compressible flows is how compressibility affects the dissipation rate of $k$ and $\omega$. A compressibility function, $F(M_t)$, is used to isolate the effects of compressibility in the $k$–$\omega$ SST model, so that the dissipation of $k$ becomes:

$$Y_k = \bar{Y}_k [1 + \zeta^* F(M_t)], \tag{7}$$

and the dissipation of $\omega$:

$$Y_\omega = \bar{Y}_\omega \left[ 1 - \frac{\beta_t^*}{\beta^*} \zeta^* F(M_t) \right], \tag{8}$$

where $\bar{Y}_k$ and $\bar{Y}_\omega$ are the dissipation of $k$ and $\omega$ for the incompressible case. The constants $\zeta^*$ and $\beta_t^*$ and function $\beta^*$ are standard in ANSYS Fluent. The function of compressibility is:

$$F(M_t) = \begin{cases} 0, & \text{if } \frac{\sqrt{2k}}{c} \leq 0.25 \\ \frac{2k}{c^2} - \frac{1}{16}, & \text{if } \frac{\sqrt{2k}}{c} > 0.25 \end{cases} \tag{9}$$

It is observed that for low values of turbulent kinetic energy, the effects of compressibility are negligible, and the dissipation rate becomes $Y_k = \bar{Y}_k$ and $Y_\omega = \bar{Y}_\omega$.

### 2.2 Numerical Methods

The numerical simulation developed in this work was based on the geometry of a real experimental nozzle, as illustrated in Fig. 1. The design strictly followed the configurations and dimensions found in industrial applications, albeit at a reduced scale, since it represents a model used in experimental bench tests. The technical drawing used as a reference for developing the geometry was provided directly to the authors for the execution of both the tests and the numerical simulations, ensuring high fidelity to the actual industrial design. The analyzed nozzle is representative of configurations widely employed in the steel industry for mass steel production, similar to the experimental one of Maia *et al.* (2017). To ensure greater computational efficiency and mesh performance, a geometric simplification was carried out by replacing the original rounded chamfer with a straight-edged chamfer. This allowed for the maintenance of mesh continuity and quality without compromising the physical fidelity of the flow.

The computational domain was designed to encompass the entire jet behavior, with dimensions of 500 mm in length and 150 mm in height, corresponding to approximately 100 and 30 times the nozzle diameter, respectively, according

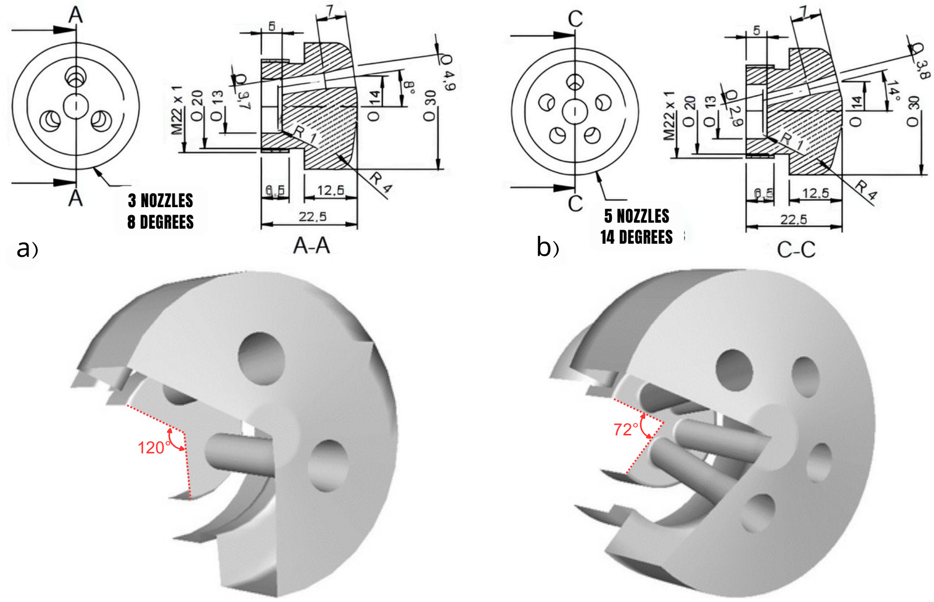


Figure 1. Three-dimensional geometries of the nozzles simulated in this study, with partial cuts for internal visualization: (a) configuration with three nozzles and (b) configuration with five nozzles, both based on industrial models and scaled to match the numerical test conditions.

to Alam *et al.* (2010). To simulate different nozzle arrangements, a geometric angle of 120° was adopted for the three-nozzle cases, allowing, through symmetry and periodicity conditions, the replication of three jets from a single nozzle, following the methodology of Garajau *et al.* (2017). For five-nozzle configurations, the domain angle was adjusted to 72°, maintaining the representativeness of the industrial arrangement. The walls of the lance and nozzle were modeled with a no-slip condition, while the lateral surfaces, highlighted in yellow in Fig 2, were assigned periodic conditions to ensure flow continuity between corresponding faces. The outer surface of the cylinder was treated with a free-slip condition, ensuring a zero tangential velocity gradient and a normal velocity component equal to zero.

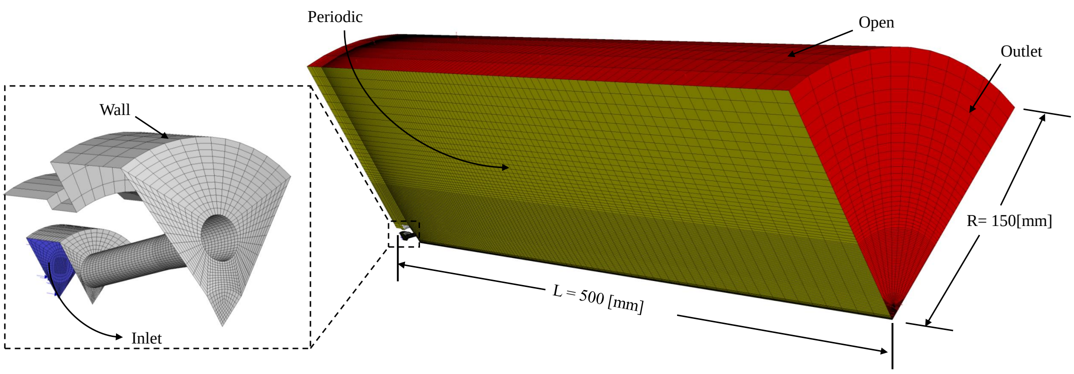


Figure 2. Representation of the computational domain, mesh structure, and boundary conditions for the CFD simulation, highlighting the constructive details of the five-nozzle configuration. The different boundaries (wall, inlet, outlet, periodic, and free) and the main dimensions adopted in the numerical tests are indicated.

The three-dimensional simulations were performed using Ansys Fluent 2025 R1, adopting symmetry conditions in the domain to optimize computational cost and processing time, an approach recommended for complex supersonic flows, as indicated by Igra *et al.* (1998) and Hadjadj *et al.* (2015).The mesh employed consisted of homogeneous hexahedral elements, selected for their high orthogonal quality. A coarse initial mesh was generated and subsequently refined adaptively in critical regions—such as zones with steep pressure and density gradients and areas where shock waves occur, which are typical of supersonic jets in Laval nozzles. This adaptive mesh refinement method was crucial for improving computational efficiency, as it allowed for increased resolution only where necessary, thereby reducing the overall number of elements and processing time without sacrificing the accuracy of the results.

The cut-cell method was employed to subdivide the original cells into different refinement levels; in three-dimensional simulations, each cell can be divided into up to $2^{3n}$ elements, where $n$ represents the maximum refinement level. Two main criteria were used to define the regions of highest refinement: cells with Mach numbers between 0.8 and 1.2, to adequately capture the supersonic core, and regions with a density ratio greater than 0.5 times the global average density, in order to accurately represent both the potential core and the shock waves.

The $SST\ k-\omega$ turbulence model was selected for its proven ability to accurately represent phenomena present in supersonic flows, including shock waves and large pressure and density gradients, and it is widely validated in the literature for this type of application (Li *et al.*, 2015). Compressibility effects were considered, assuming air as an ideal gas, and all fluid properties as well as the numerical methods employed are detailed in Table 1. The basic operational parameters adopted, such as inlet relative pressure of 11 atm, temperature of 300 K, nozzle pressure ratio (NPR) equal to 12, and outlet pressure of 0 atm, follow the industrial standard for BOF converter operations and are also detailed in Table 1. The numerical approach included implicit methods, pressure-velocity coupling via the COUPLED algorithm, and third-order spatial discretization for density and momentum, ensuring accuracy and stability in the simulations.

Table 1. Fluid properties and numerical methods applied to the simulations.

| | | | |
|---|---|---|---|
| **Material (Air)** | Density at ambient temperature ($\rho_0$) | | 1.225 kg/m$^3$ |
| | Specific heat at constant pressure ($c_p$) | | 1006.43 J/kg·K |
| | Molecular viscosity ($\mu$) | | $1.7897 \times 10^{-5}$ Pa·s |
| | Molecular weight ($M$) | | 28.966 kg/kmol |
| | Thermal conductivity ($\lambda$) | | 0.0242 W/m·K |
| **Solution Methods** | Pressure-Velocity Coupling | | Coupled |
| | **Spatial Discretization** | Gradient | Least Squares Cell Based |
| | | Pressure | Second Order |
| | | Momentum | Third-order MUSCL |
| | | Density | Third-order MUSCL |
| | | Energy | Second Order Upwind |
| | | Turbulent kinetic energy ($k$) | Second Order Upwind |
| | | Specific dissipation rate ($\omega$) | Second Order Upwind |

Finally, the choice of adaptive mesh and symmetry conditions significantly reduced computational cost without losing the ability to capture relevant physical phenomena, such as the complex interaction between multiple jets, flow regimes ranging from subsonic to supersonic, shock wave formation, recirculation zones, and flow separation. Therefore, the adopted methodology ensures the representativeness of the results for industrial applications while maintaining computational feasibility for parametric and comparative studies between different nozzle geometries.

## 3. RESULTS AND DISCUSSIONS

Although $SST\ k-\omega$ turbulence model provides good results for supersonic flows, wall interactions, and strong pressure gradients, it has limitations that should be considered when interpreting the results. Being based on Reynolds-Averaged Navier–Stokes (RANS) equations, it does not capture instantaneous fluctuations or fine details of turbulent structures, which may lead to a smoothing of phenomena such as the dynamic coalescence of multiple jets. Furthermore, its performance depends on empirical constants calibrated for specific conditions, which can cause deviations under flow regimes significantly different from the reference ones. In free-flow regions or in cases of strong jet interaction, the model may overestimate or underestimate dissipation, and therefore its accuracy is also tied to mesh quality and refinement. Thus, although robust and widely validated, it is recommended to interpret the results with caution when extrapolating to extreme conditions, and to complement them with experiments or more advanced models when aiming to capture highly transient and nonlinear phenomena.

The simulations initially underwent a validation process, based on comparative studies between numerical simulations and experiments available in the literature, with emphasis on the characteristic physical phenomena of supersonic jets in convergent-divergent nozzles. For this procedure, density gradient contours were simulated for two distinct values of nozzle pressure ratio (NPR), as adopted in the experiment by Zapryagaev *et al.* (2002). The numerical results obtained were compared with experimental data, as illustrated in the works of Zotelle *et al.* (2024) and Garcia *et al.* (2024). The analysis demonstrated that the employed numerical model was able to reproduce the jet behavior with good accuracy, validating its application in the simulations proposed in this study.

Furthermore, the aforementioned authors performed a mesh independence test using five refinement levels (n = 0 to n = 4), based on simulations employing Schlieren images. It was observed that the initial levels (n = 0 and n = 1) did not adequately capture some flow features. From level n = 2, the main structures began to be visualized, although there was still a lack of details near the nozzle exit. Since levels n = 3 and n = 4 presented similar results, but with a significant increase in the number of elements and, consequently, in computational cost, level n = 3 was chosen as the most suitable for the simulations.

Based on the validation for BOF simulations and employing the models and parameters previously described, the results obtained reveal important aspects, such as the variation of mass flow rate as a function of the nozzle pressure ratio (NPR) and the nozzle configuration for the analyzed geometries. These findings also highlight the influence of these parameters on the length of the supersonic core of the jet.

Figure 3 illustrates the shock wave patterns observed in Laval nozzles and the corresponding variation in the potential core length for both three- and five-nozzle configurations, under different NPR conditions. It is evident from the image that, for all NPR values analyzed (4, 8, and 12), the increase in the jet core length is more pronounced for the three-nozzle geometry compared to the five-nozzle configuration. This suggests that, while both geometries exhibit an extension of the supersonic core with increasing NPR, the effect is consistently greater in the three-nozzle case, resulting in longer and more defined core regions.

This behavior is consistent across all simulated pressure ratios and underscores the fundamental role of nozzle geometry in determining the jet structure and its potential for penetration and mixing within the molten bath. The visualization of shock cells and the extent of the potential core in these simulations provide a solid basis for understanding how design choices impact the efficiency and dynamics of the BOF process.

The shock wave images (Schlieren) indicate that, in the five-nozzle configuration, the jets tend to coalesce shortly after exiting the nozzles. In contrast, in the three-nozzle configuration, the jets remain more open, exhibiting less interaction between them.

This behavior can be explained by the increase in the number of nozzles and the reduction of the angle between them, which causes the jets to be launched closer to each other, facilitating their convergence toward the central axis of the lance. The coalescence phenomenon is accentuated especially when the inclination angle of the nozzles is reduced, as evidenced by recent research: the smaller the angle, the greater the mutual interaction and the propensity for jet coalescence. As a consequence, there is a central region with lower static pressure, which attracts the jets to the center, favoring the meeting and merging of the flows (Maia *et al.*, 2017).

In the literature, Li *et al.* (2015) and other authors emphasize that the coalescence of jets in multi-nozzle lances is a beneficial phenomenon for increasing penetration and metallurgical efficiency, as long as there is no excess concentrated energy that could lead to localized wear. For example, the study by Li *et al.* (2015) indicates that coalescence is facilitated by smaller angles between the nozzles and by a lower number of nozzles. However, when the number of nozzles increases (to four or five), coalescence occurs closer to the nozzle exit, resulting in a shorter supersonic core, but with a larger impact area and a more efficient energy distribution.

Furthermore, research such as that by Willis *et al.* (2022) corroborates, through Schlieren images, that the coalescence of wave fronts in supersonic jets leads to more complex shock structures, as well as increased mixing intensity and momentum transfer near the central axis. This is consistent with the observations from the simulations: in the five-nozzle configuration, the shock waves overlap and the jets merge rapidly. Conversely, in the three-nozzle configuration, the jets follow more independent trajectories, with less overlap and a longer supersonic core length.

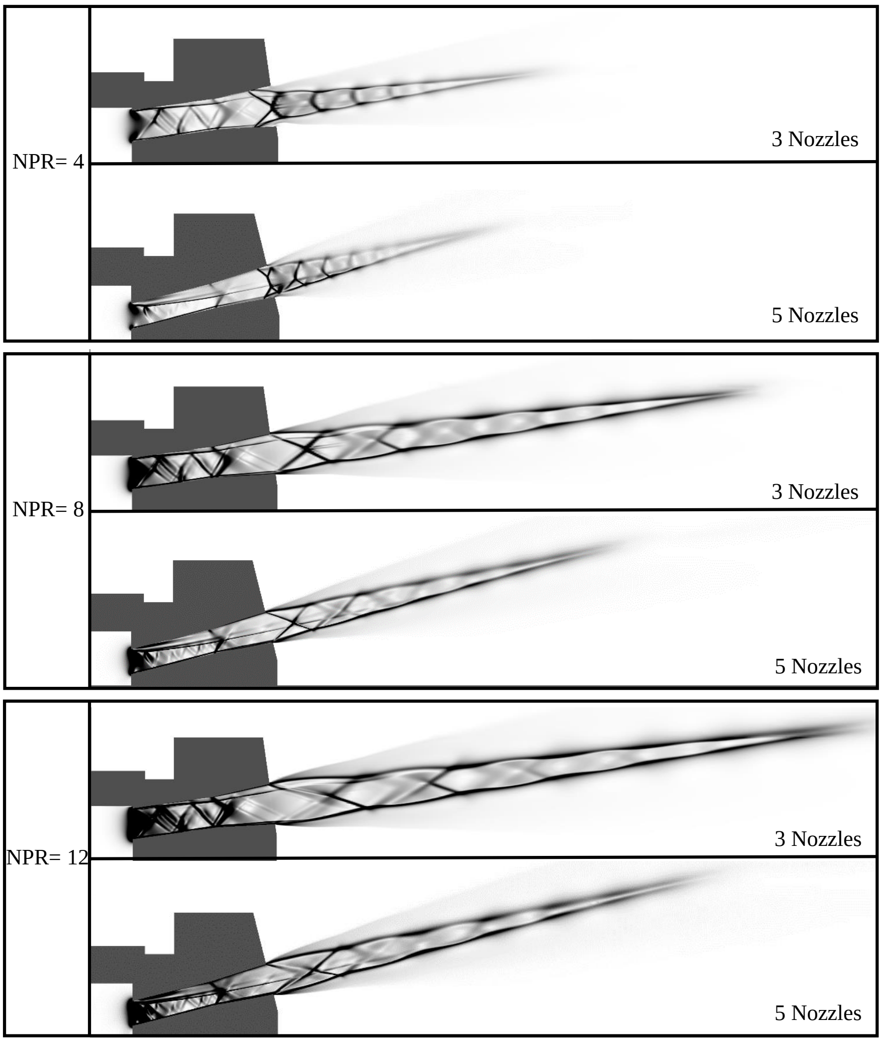


Figure 3. Comparison of simulated Schlieren images showing the density gradients in the supersonic jet regions for different nozzle pressure ratios (NPR = 4, 8, and 12) in the three- and five-nozzle configurations. The visualizations highlight the shock wave pattern, potential core length, and degree of jet coalescence as a function of geometry and pressure variation.

To quantitatively assess the mass flow associated with the results presented, the Reports > Fluxes > Mass Flow Rate function was used, which enables the software to compute the mass balance across a specified region. The mass flow rate values obtained through this method are presented in Figure 4, allowing for a direct comparison of the influence of nozzle configuration and NPR on the resulting flow rates.

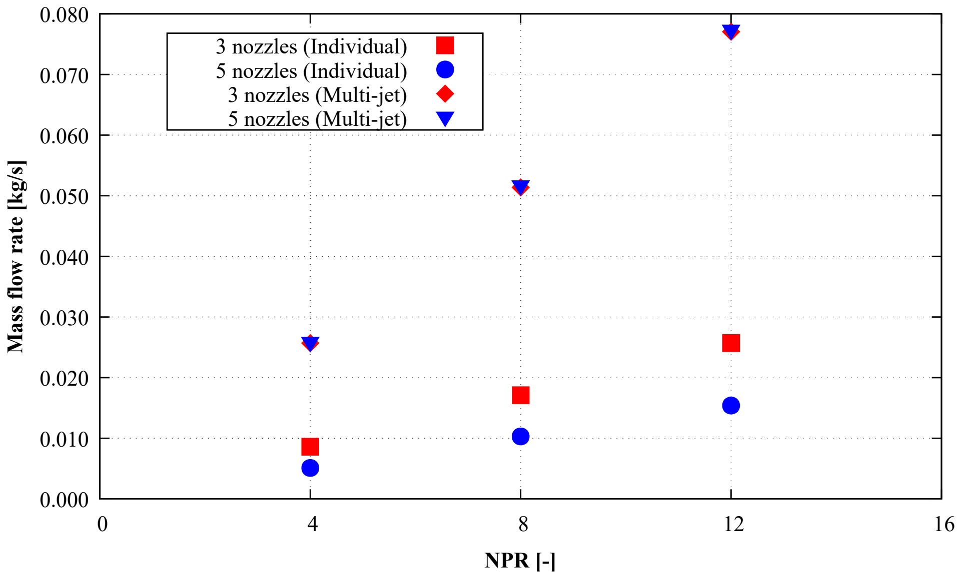


Figure 4. Variation of mass flow rate as a function of the nozzle pressure ratio (NPR) for three- and five-nozzle configurations, considering both individual-jet analysis and the multi-jet system. The results show the combined increase in total mass flow rate with a greater number of outlets, as well as the direct influence of NPR on jet performance.

Regarding the graphical data, it is observed that the total mass flow rate is substantially higher in lances with multiple jets compared to individual jets, while maintaining the same NPR value, for both 3- and 5-nozzle configurations. Additionally, in both scenarios, an increase in the number of nozzles (to 3 and 5) results in a further increment in the total mass flow rate. This finding is consistent with the literature and recent experiments, as highlighted by Garcia *et al.* (2023a).

The specialized literature emphasizes that the use of lances with multiple nozzles not only increases the total oxygen mass flow rate at the outlet but also modifies the flow pattern. This change promotes greater jet dispersion, optimizing operational control and mitigating undesirable effects such as slopping and refractory wear. Studies such as that of Ji *et al.* (2021) indicate that the interaction between multiple jets can foster both coalescence and deflection of the jets toward the central axis. This, in turn, expands the impact area and favors more efficient mixing in the metal bath. Similarly, Miura *et al.* (2024) confirm that increasing the number of nozzles contributes to the reduction of slag foaming height, which improves the stability of the steelmaking process.

Recently, several studies have indicated that the geometry and angle of the nozzles exert a direct influence on the length of the supersonic core, jet penetration, and blowing efficiency in the metal bath. Although multi-outlet nozzles tend to present shorter potential cores, they compensate with a larger impact area and superior energy distribution. This characteristic is highly desirable to avoid localized wear and to extend equipment lifespan, as evidenced by Silveira *et al.* (2019).

Following this previously mentioned trend, Figure 5 clearly illustrates how this increase in NPR directly impacts the length of the supersonic core of the jet for both nozzle geometries. The graph clearly shows that, for both cases analyzed (3 and 5 nozzles), the increase in NPR results in a more extensive supersonic core length. However, it is worth noting that this increase is significantly more pronounced in the three-nozzle configuration, whose core length values are consistently higher than those observed for five nozzles at all evaluated NPR levels.

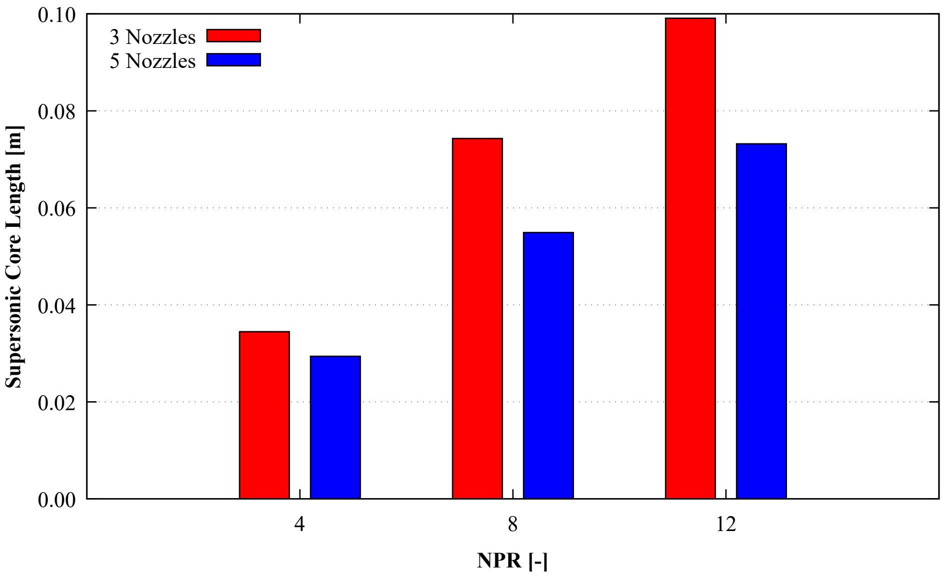


Figure 5. Variation of mass flow rate as a function of the nozzle pressure ratio (NPR) for three- and five-nozzle configurations, considering both individual-jet analysis and the multi-jet system. The results show the combined increase in total mass flow rate with a greater number of outlets, as well as the direct influence of NPR on jet performance.

This difference can be attributed to the fact that, although the five-nozzle geometry provides a total mass flow similar to that of three nozzles, the jet energy is distributed among more outlets, resulting in shorter potential cores and a wider impact area, as discussed in the literature (Silveira *et al.*, 2019); (Miura *et al.*, 2024). On the other hand, the three-nozzle configuration concentrates the blowing energy into fewer jets, favoring the formation of a longer supersonic core and, consequently, greater penetration into the metal bath. This aspect is fundamental for processes that require greater metallurgical efficiency, as pointed out in previous results and highlighted.

Therefore, the integrated analysis of mass flow data and supersonic core length shows that the choice of the number of nozzles should consider the balance between productivity, mixing efficiency, and operational control. While multiple nozzles favor higher flow rates and energy distribution, a smaller number of nozzles promotes longer cores and deeper penetration, with the final decision depending on the specific needs of the BOF process and operational optimization strategies.

## 4. CONCLUSIONS

Therefore, based on the comprehensive numerical analysis carried out in this study, it was confirmed that both the geometry and the number of nozzles have a direct and significant influence on the mass flow rate and the length of the supersonic core of jets in BOF converters. It was observed that three-nozzle configurations favor the formation of longer cores and, consequently, greater jet penetration, while five-nozzle configurations provide higher total flow and better energy distribution, contributing to greater operational control and reduced risks such as refractory wear and slopping. These findings, which are consistent with recent literature, reinforce the importance of carefully selecting constructive and operational parameters to optimize metallurgical performance and process safety. For future work, it is recommended to extend the investigation to geometries with an even greater number of nozzles and to conduct detailed experimental comparisons, aiming at the continuous improvement of industrial practices in steelmaking.

## 5. ACKNOWLEDGEMENTS

This work was carried out with support from Espírito Santo Research and Innovation Support Foundation (Fapes - Fundação de Amparo à Pesquisa e Inovação do Espírito Santo) –T.O. 1052/2022. The authors also thank Fapes for the grant funding that enabled this study to be conducted.

## 6. REFERENCES

, 2024. *ANSYS Fluent User's Guide*. ANSYS Inc. Release 2024R1.

Alam, M., Naser, J. and Brooks, G., 2010. "Computational fluid dynamics simulation of supersonic oxygen jet behavior at steelmaking temperature". *Metallurgical and Materials Transactions B*, Vol. 41, pp. 636–645.

Feng, C., Zhu, R., Dong, K., Wei, G., Han, B., Li, W. and Wu, W., 2021. "Effects of nozzle layout and parameters on the jet characteristics of a co 2+ o 2 mixed oxygen lance". *Metallurgical and Materials Transactions B*, Vol. 52, pp. 425–439.

Garajau, F.S., Guerra, M., Maiaa, B., Cetlinb, P. and Moreira, D.A., 2017. "Case study: Wear in supersonic nozzle of tip lance in vallourec brazil steelmaking". *AISTech 2017 Proceedings: AISTech 2017 Proceedings*, pp. 1365–1375.

Garcia, P.F., Zotelle, A.C., Siqueira, R.N., Barbosa, J.P., Maia, B.T. and Oliveira, J.R., 2023a. "Numerical analysis of the effects of convergent-divergent nozzle geometry on the characteristics of supersonic jet in bof converters". In *Proceedings of the 27th International Congress of Mechanical Engineering (COBEM 2023)*. pp. 1–10.

Garcia, P.F., Basilio, L.M., Zotelle, A.C., Maia, B.T., Barbosa, J.P., de Oliveira, J.R. and do Nascimento Siqueira, R., 2023b. "Effects of nozzle pressure ratio on supersonic flow startup structures and their consequences on bof steel making process". *Proceedings of 52º Steelmaking & Non-Ferrous Metal, ABM Week*.

Garcia, P.F., Zotelle, A.C., do Nascimento Siqueira, R., Barbosa, J.P., de Oliveira, J.R. and Maia, B.T., 2024. "Three-dimensional simulation of supersonic nozzle start-up structures and their consequences on the bof steelmaking process". *Proceedings of the Iron & Steel Technology Conference (AISTech 2024)*.

Hadjadj, A., Perrot, Y. and Verma, S., 2015. "Numerical study of shock/boundary layer interaction in supersonic overexpanded nozzles". *Aerospace science and technology*, Vol. 42, pp. 158–168.

Igra, O., Wang, L., Falcovitz, J. and Amann, O., 1998. "Simulation of the starting flow in a wedge–like nozzle". *Shock Waves*, Vol. 8, pp. 235–242.

Ji, X., Liu, Y., Wang, Z., Zhang, Y. and Li, J., 2021. "Effect of the jet from top lance on slag foaming behavior in basic oxygen furnace steelmaking". *ISIJ International*, Vol. 61, No. 9, pp. 1396–1404. doi:10.2355/isijinternational.ISIJINT-2024-068. URL `https://www.jstage.jst.go.jp/article/isijinternational/64/9/64`$_ISIJINT - 2024 - 068/_html/ - char/en$.

Li, M., Li, Q., Kuang, S. and Zou, Z., 2015. "Coalescence characteristics of supersonic jets from multi-nozzle oxygen lance in steelmaking bof". *Steel research international*, Vol. 86, No. 12, pp. 1517–1529.

Li, M., Li, Q., Li, L., He, Y. and Zou, Z., 2014. "Effect of operation parameters on supersonic jet behaviour of bof six-nozzle oxygen lance". *Ironmaking & Steelmaking*, Vol. 41, No. 9, pp. 699–709.

Maia, B.T., Martins, A.A. and Nascimento, R.D.R., 2017. "Analysis of geometrical aspects of bof converters and correlations with process parameters". *Revista Matéria*, Vol. 28, No. 1, p. e13865.

Maia, B.T., Santos, B.O.d.A., Garajau, F.S. and Guerra, M.d.S.L., 2014. "Simulações numéricas da vazão de água em lanças para bof". In *Seminário de Aciaria – Internacional, 45.* ABM, Porto Alegre, pp. 1–12. Anais.

Miura, K., Sato, T., Nakamura, S. and Yamamoto, K., 2024. "Effect of the jet from top lance on slag foaming behavior in basic oxygen furnace steelmaking". *ISIJ International*, Vol. 64, No. 9, pp. 1396–1404. doi:10.2355/isijinternational.ISIJINT-2024-068. URL `https://www.jstage.jst.go.jp/article/isijinternational/64/9/64`$_ISIJINT - 2024 - 068/_html/ - char/en$.

Silveira, D., Hamadeh, H., Pastel, K., Huber, J.C. and Brosse, G., 2019. "Effect of supersonic nozzle design on jet behavior in bof steelmaking". In *50º Seminário de Aciaria, Fundição e Metalurgia de Não-Ferrosos — ABM Week 2019*. São Paulo, SP, Brazil. URL `https://abmproceedings.com.br/en/article/download-pdf/effect-of-supersonic-nozzle-design-on-jet-behav`

Willis, W.A. *et al.*, 2022. "Analysis of spark-generated waveforms coalescing in air using schlieren imaging". *Journal of the Acoustical Society of America*, Vol. 151, No. 2, p. A120. doi:10.1121/10.0010792.

Yaravintelimath, A., Raghunandan, B. and Moríñigo, J.A., 2016. "Numerical prediction of nozzle flow separation: Issue of turbulence modeling". *Aerospace Science and Technology*, Vol. 50, pp. 31–43.

Zapryagaev, V.I., Kudryavtsev, A.N., Lokotko, A.V., Solotchin, A.V. and Hadjadj, A., 2002. "An experimental and numerical study of a supersonic-jet shock-wave structure". *NASA STI/Recon Technical Report N*, Vol. 3, p. 12803.

Zotelle, A.C., Garcia, P.F., do Nascimento Siqueira, R., Barbosa, J.P., de Oliveira, J.R. and Maia, B.T., 2024. "Influence of geometry on flow patterns and metal accumulation at the lance tip in bof converters". In *AISTech 2024 - Proceedings of the Iron & Steel Technology Conference*. Association for Iron & Steel Technology, Columbus, Ohio, USA, pp. 624–635. doi:10.33313/388/065.

## 7. RESPONSIBILITY NOTICE

The authors are the only responsible for the printed material included in this paper